Experimental Parasitology 158 (2015) 31–41

Contents lists available at ScienceDirect

Experimental Parasitology

journal homepage: www.elsevier.com/locate/yexpr

Full length article

A confocal microscopy-based atlas of tissue architecture in the tapeworm *Hymenolepis diminuta*

Tania Rozario, Phillip A. Newmark *

Howard Hughes Medical Institute, Department of Cell and Developmental Biology, University of Illinois at Urbana-Champaign, Urbana, IL, USA

HIGHLIGHTS

- Lectins, antibodies and common stains specifically label different tapeworm tissues.
- An atlas of *Hymenolepis diminuta* organs was constructed using confocal microscopy.
- This work will facilitate phenotypic characterization after genetic perturbation.

GRAPHICAL ABSTRACT

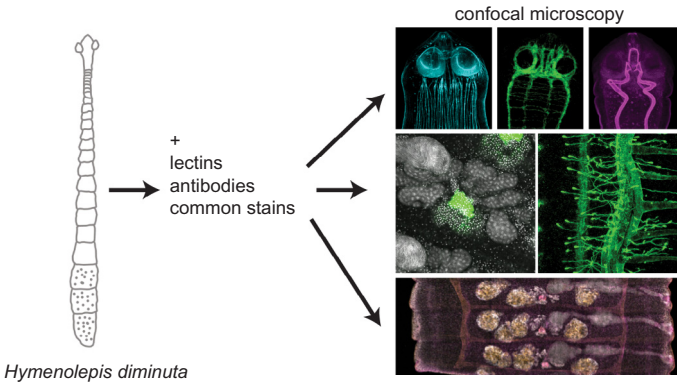

ARTICLE INFO

Article history:
Received 22 December 2014
Received in revised form 14 May 2015
Accepted 27 May 2015
Available online 3 June 2015

Keywords:
Tapeworm
Cestoda
Hymenolepis diminuta
Lectin
Platyhelminthes
Flatworm

ABSTRACT

Tapeworms are pervasive and globally distributed parasites that infect millions of humans and livestock every year, and are the causative agents of two of the 17 neglected tropical diseases prioritized by the World Health Organization. Studies of tapeworm biology and pathology are often encumbered by the complex life cycles of disease-relevant tapeworm species that infect hosts such as foxes, dogs, cattle, pigs, and humans. Thus, studies of laboratory models can help overcome the practical, ethical, and cost-related difficulties faced by tapeworm parasitologists. The rat intestinal tapeworm *Hymenolepis diminuta* is easily reared in the laboratory and has the potential to enable modern molecular-based experiments that will greatly contribute to our understanding of multiple aspects of tapeworm biology, such as growth and reproduction. As part of our efforts to develop molecular tools for experiments on *H. diminuta*, we have characterized a battery of lectins, antibodies, and common stains that label different tapeworm tissues and organ structures. Using confocal microscopy, we have assembled an "atlas" of *H. diminuta* organ architecture that will be a useful resource for helminthologists. The methodologies we describe will facilitate characterization of loss-of-function perturbations using *H. diminuta*. This toolkit will enable a greater understanding of fundamental tapeworm biology that may elucidate new therapeutic targets toward the eradication of these parasites.

* Corresponding author. Fax: +1 217 244 1648.
E-mail address: pnewmark@illinois.edu (P.A. Newmark).

http://dx.doi.org/10.1016/j.exppara.2015.05.015
0014-4894/

1. Introduction

Tapeworms (Platyhelminthes, Cestoda) cause a variety of diseases in both humans and livestock. Larval tapeworms of the family Taeniidae are the etiological agents of hydatid disease and cysticercosis, which cause a range of debilitating pathologies such as organ failure and seizures that can be fatal (Brunetti et al., 2010; Eckert and Deplazes, 2004; Garcia et al., 2007). Adult tapeworms from all genera almost exclusively reside in the intestine and cause milder symptoms than their larval counterparts, such as abdominal discomfort and diarrhea (Craig and Ito, 2007). Tapeworms are pervasive and globally distributed, with a human disease burden estimated at 1 million disability-adjusted life years (Budke et al., 2009).

Twelve tapeworm genomes have been sequenced and are publically available (Wellcome Trust Sanger Institute, 2014; Tsai et al., 2013). This wealth of genomic data will facilitate the use of comparative bioinformatics to identify potential targets for designing anthelminthic drugs. To complement the genome sequencing efforts, it is necessary to establish tractable model systems to elucidate the functions of parasite genes. In this respect, rodent tapeworms of the genus *Hymenolepis* are convenient laboratory models with many practical advantages (Cunningham and Olson, 2010; Pouchkina-Stantcheva et al., 2013; Siles-Lucas and Hemphill, 2002). The rat intestinal tapeworm *Hymenolepis diminuta* is especially suited for the study of parasite biology in part because the complete life cycle can be recapitulated *in vivo* and *in vitro* (Evans, 1980; Roberts, 1980; Ubelaker, 1980). Studies on *H. diminuta* will enable us to investigate the genetic regulation of tapeworm growth and reproduction, which is potentially applicable to a wide range of disease-relevant flatworms that are more difficult to rear and manipulate. However, modern molecular tools such as RNA *in situ* hybridization and loss-of-function perturbations need to be developed to fully realize the potential of *H. diminuta* as a model system. These efforts are ongoing in our lab.

In this study, we characterize a battery of common reagents, including plant lectins and antibodies with broad cross-reactivity, and develop an easily adaptable whole-mount staining protocol. These markers have allowed us to use confocal microscopy to reveal an "atlas" of different tissues and organ structures of *H. diminuta*. We chose this set of stains because they have been shown to label various tissues of other flatworms, namely the parasitic blood fluke *Schistosoma mansoni* (Collins et al., 2011) and the free-living planarian *Schmidtea mediterranea* (Chong et al., 2011; Zayas et al., 2010). These stains serve as convenient tools for cross-species studies using multiple flatworms. More importantly, these stains will be valuable tools to investigate phenotypes following loss-of-function perturbations.

2. Materials and methods

2.1. Obtaining adult H. diminuta

Mealworm beetles (*Tenebrio molitor*) carrying *H. diminuta* cysticercoids were purchased from Carolina Biological. Cysticercoids were dissected out in 0.85% NaCl and fed to Sprague–Dawley rats by oral gavage. Adult tapeworms were recovered between 6 and 21 days after infection. To recover the adults, the rats were euthanized in a CO_2 chamber and the small intestine removed. The contents of the intestine were flushed out with Hanks Balanced Salt Solution (HBSS) (Life Technologies) (140 mg/L $CaCl_2$, 100 mg/L $MgCl_2$.6H2O, 100 mg/L $MgSO_4$.7H_2O, 400 mg/L KCl, 60 mg/L KH_2PO_4, 350 mg/L $NaHCO_3$, 8 g/L NaCl, 48 mg/L Na_2HPO_4, 1 g/L D-glucose, no phenol red). The tapeworms were washed by transferring them into fresh HBSS several times using a stainless steel tool with a hooked end (Moody Tools).

2.2. Excystment of H. diminuta

Cysticercoids were dissected from infected *T. molitor* and treated with acid-pepsin (10 mg/mL pepsin (Sigma) in 0.85% NaCl pH 2.0) for 10 min at 37 °C. Cysticercoids were then transferred to bile solution (10 mg/mL sodium tauroglycocholate (HiMedia), 5 mg/mL trypsin (Sigma), in HBSS pH 7.4) for 30 min at 37 °C; more than 80% of cysticercoids excysted following this protocol. Juveniles were washed in HBSS. All Petri dishes were pre-coated with 0.5% bovine serum albumin (BSA) to inhibit the cysticercoids and juveniles from sticking.

2.3. Fixation and staining

Adult *H. diminuta* were heat-killed by extending the worms in 70–75 °C distilled water for ~5 s to straighten them. The worms were then immediately fixed in 4% formaldehyde/0.1% NP40/PBSTx (PBS (8 g/L NaCl, 200 mg/L KCl, 270 mg/L KH_2PO_4, 1.42 g/L Na_2HPO_4, pH 7.4) + 0.3% Triton-X 100) for 2 hours at room temperature or overnight at 4 °C. Adult worms range from 5 to 40 cm in length depending on their age. After fixation they were rinsed in PBSTx and cut into ~0.5 cm pieces. Samples were dehydrated into ethanol and stored at –20 °C until use. Rehydrated samples were treated with Proteinase K (Invitrogen) solution (2 μg/mL, 0.1% SDS in PBSTx) for 20 min–1 hr depending on the size of the samples and then post-fixed for 10 min in 4% formaldehyde/PBSTx. Proteinase K treatment was not necessary for most stains and should be omitted for staining with anti-synapsin antibodies and phalloidin. Samples were blocked in 0.6% BSA (Jackson Immuno Research)/0.45% Fish Gelatin (Sigma)/5% Horse Serum (Sigma)/PBSTx. All primary stains were done in blocking solution overnight at 4 °C.

For a list of primary stains used with corresponding dilutions, refer to Supplementary Table S1. The phalloidin and lectins were pre-conjugated to fluorophores. For antibody staining we used tyramide signal amplification (TSA) with in-house FAM-, TAMRA-, or DyLight 633-conjugated tyramides (King and Newmark, 2013). TSA detection was done using secondary HRP-conjugated antibodies (Invitrogen) at 1:1000 for 2 hours at room temperature followed by 10 min incubation in Amplification Diluent containing the appropriate fluorescent tyramide (1:500 FAM- or TAMRA-tyramide or 1:250 DyLight 633-tyramide, 0.003% H_2O_2, 20 μg/mL 4-iodophenylboronic acid in dimethylformamide, in TSA buffer (2 M NaCl, 100 mM borate, pH 8.5, stored at 4 °C)). DAPI staining was performed in PBSTx at 1 μg/mL overnight at 4 °C. All samples were cleared in 80% glycerol/10 mM Tris pH 7.5/1 mM EDTA and mounted on slides for imaging.

Newly excysted juvenile *H. diminuta* were very small and difficult to track. Thus, staining was done in 1.7 mL Eppendorf tubes pre-coated with 0.5% BSA. Before every solution change, the tubes were microcentrifuged for ~10 s to accumulate the juveniles to the bottom. Then ~95% of the supernatant was removed for every wash. Dehydration and Proteinase K treatment were omitted.

2.4. Imaging

Samples were imaged on a Zeiss LSM 710 confocal microscope (Carl Zeiss). Objectives used: EC Plan-Neofluar 10×/0.3, Plan-Apochromat 20×/0.8, C-Apochromat 40×/1.2 water, and Plan-Apochromat 63×/1.4 Oil. Alexa 488/FITC/FAM, TAMRA/Rhodamine, and DyLight 633 fluorophores were excited with 488 nm, 561 nm, and 633 nm lasers, respectively. Image processing was done using Zen 2009 (Carl Zeiss) or ImageJ.

3. Results and discussion

In this paper, we employ common stains, lectins, and antibodies to observe and characterize the organization of numerous tissues in adult *H. diminuta*. Our goal is to illustrate that the majority of adult tapeworm tissues can be observed using simple staining methods and reagents, making this species amenable to laboratory manipulations. Our observations concur with previous descriptions of *H. diminuta* anatomy using electron microscopy and histology. For a more in-depth description of *H. diminuta* ultrastructure, readers are referred to an excellent review by Lumsden and Specian (1980).

3.1. General adult body plan and life cycle

3.1.1. Body plan organization

Adult *H. diminuta* can be divided into three parts: scolex, germinative region or neck, and strobila (Fig. 1). The scolex is the most anterior structure, made of a centrally protruding hookless rostellum and four muscular suckers. The neck is directly posterior to the scolex and serves as a growth zone from which the strobila is formed (Bolla and Roberts, 1971; Lumsden and Specian, 1980). The strobila consists of hundreds to thousands of apparent segments called proglottids. There is no internal septum or barrier that separates each proglottid. The proglottids "bud" one at a time from the neck; consequently, the most anterior proglottids are the youngest and the most posterior proglottids are the oldest. Each proglottid is fated to specify and elaborate the entire complement of male and female reproductive organs. Following fertilization, embryos are stored in the uterus in each proglottid. Toward the posterior of the worm, the oldest proglottids become gravid. In each gravid proglottid, the uterus expands to accommodate developing embryos while other reproductive structures degenerate.

H. diminuta reaches reproductive maturity in 2–3 weeks and can remain healthy and reproductively active inside the rat intestine for the duration of the rat's lifespan. In this time, *H. diminuta* reaches an equilibrium length of ~60 cm and roughly 2000 proglottids (Chandler, 1939; Roberts, 1961).

3.1.2. Life cycle

H. diminuta cannot complete its life cycle within a single host. Once the adult has reached gravidity, gravid proglottids are pinched off and expelled out of the host rat, inside the stool. The embryos within the shed proglottids must be eaten by a suitable arthropod host (such as beetles), in which larval stages of development occur. Larval development has been extensively reviewed in Ubelaker (1980). In our laboratory, gravid proglottids are fed to mealworm beetles (*T. molitor*), which facilitate development of infective cysticercoids in 8–14 days (Voge and Heyneman, 1957). The infective cysticercoids can remain dormant in the hemocoel for the life of the beetle or until the infected beetle is consumed by a rat. To complete the life cycle in the laboratory, cysticercoids are dissected out of the beetles and administered to rats via oral gavage. When the cysticercoids reach the stomach, excystment of the juvenile tapeworm is triggered and the empty cyst is discarded (Rothman, 1959). Newly excysted juvenile tapeworms possess a scolex and a short body with no strobila. The juvenile establishes itself in the rat intestine using its suckers to attach to the intestinal wall where it grows to reproductive maturity.

3.1.3. Major organ structures

H. diminuta, like many parasites, has reduced its genome size (Olson et al., 2012; Tsai et al., 2013) and simplified its body plan while maximizing fitness in the host environment. Tapeworms have evolved unique structures and strategies that facilitate their parasitic needs. Like all tapeworms, *H. diminuta* is devoid of an internal gut. Nutrients are absorbed and waste is excreted using a highly specialized external surface called the tegument, which is unique to parasitic flatworms. The tegument functions as both the parasite skin and gut. Furthermore, the tegument is decorated with fine projections called microtriches (Lumsden, 1975a, 1975b).

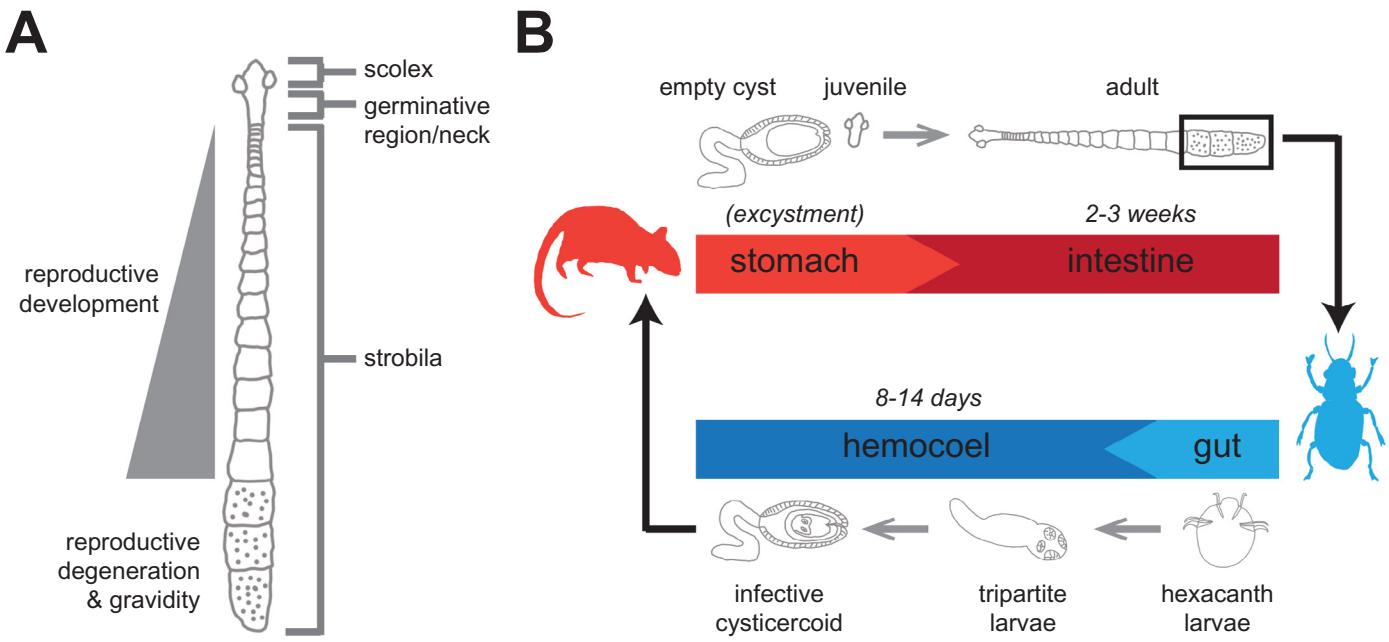

Fig. 1. Overview of the *H. diminuta* adult body plan and life cycle. (A) *H. diminuta* adults possess a scolex, germinative region/neck, and strobila. The scolex contains a rostellum and four suckers. The strobila is composed of hundreds to thousands of apparent segments known as proglottids that bud from the germinative region one at a time. Reproductive maturation progresses in an anteroposterior gradient. A mature worm undergoes fertilization and accumulates embryos inside the uterus of the terminal proglottids. The posterior proglottids that are primarily composed of embryos are termed gravid. (B) Depiction of the life cycle of *H. diminuta*.

In addition to unique parasite-specific structures such as the tegument, *H. diminuta* possesses many tissues shared by most bilaterians such as a nervous system, musculature, and osmoregulatory system. The chief difference is that many tissues that would normally be formed of epithelia are instead syncytial (Lumsden and Specian, 1980). This is the case for most of the lumenal ducts, the uterus, and the tegument.

3.2. Musculature

After excystment, each juvenile *H. diminuta* has already formed one rostellum and four suckers. These structures are highly muscularized and can be visualized by staining with phalloidin (Fig. 2A). The suckers and rostellum are retained as the tapeworm matures (Fig. 2B) and are the dominant muscular structures in the anterior of the worm. The musculature is composed of longitudinal, transverse and circular muscle fibers that have been thoroughly described using ultrastructural methods (Lumsden and Byram, 1967; Specian and Lumsden, 1980) and can be identified using phalloidin staining (Supplementary Movie S1).

The body wall musculature is circumferential and closely juxtaposed to the tegument. The strobila musculature can be defined anatomically as two cortical sheets: superficial muscle and medullary muscle, between which lie the tegumentary cytons. The superficial muscle is composed of fine fibers that form basal to the distal cytoplasm of the tegument (Fig. 2C, D) and consists of both longitudinal and circular fibers (Fig. 2E, E′). The circular fibers of the superficial muscle are weakly stained by phalloidin compared to the longitudinal fibers. The medullary muscle is made of thick fibers that are positioned basal to the tegumentary cytons (Fig. 2D, F, F′). Longitudinal medullary fibers are the most visible muscle components stained by phalloidin along the length of the worm (Fig. 2F). Cortical transverse fibers mark the proglottid boundaries (Fig. 2F′, G). In addition to the body wall musculature, phalloidin also marks the contractile elements associated with the genitalia (Fig. 2G: asterisks).

The nuclei of individual muscle cells are offset and connected by a cytoplasmic bridge (Lumsden and Byram, 1967). This organization is common to most if not all flatworms (Lumsden and Byram, 1967). The musculature is essential to tapeworm physiology as muscle contraction is used for locomotion in the intestine, attachment to the intestinal wall, and mating. Muscle cells are also used for glycogen storage (Lumsden and Specian, 1980).

3.3. Nervous system and other sensory structures

Like other flatworms, adult *H. diminuta* possesses a nervous system with both central and peripheral components. The nervous system can be visualized by staining with anti-synapsin antibodies (Fig. 3A–D), which has been previously used to describe the nervous system of multiple flatworm species (Collins et al., 2011; Fraguas et al., 2014). The “brain”, known as the cephalic ganglia, is positioned at the base of the suckers (Fig. 3A, B). Two lateral nerve cords and two median nerves originate from the cephalic ganglia and extend along the anteroposterior axis (Fig. 3A–D). The overall architecture of the cephalic ganglia and lateral nerve cords is already present in newly excysted juvenile tapeworms (Fig. 3A) and continues to increase in complexity as the animal develops.

The cephalic ganglia are made of two large laterally positioned ganglia that are connected by a transverse commissure. Anterior projections are made from the cephalic ganglia to the suckers and rostellum (Fig. 3A, B). Neuronal projections can be seen in the rostellar capsule and throughout the suckers. While synapsin staining is an excellent broad neuronal marker, it is not sufficient to represent the true diversity of neuronal connections that exist in *H.*

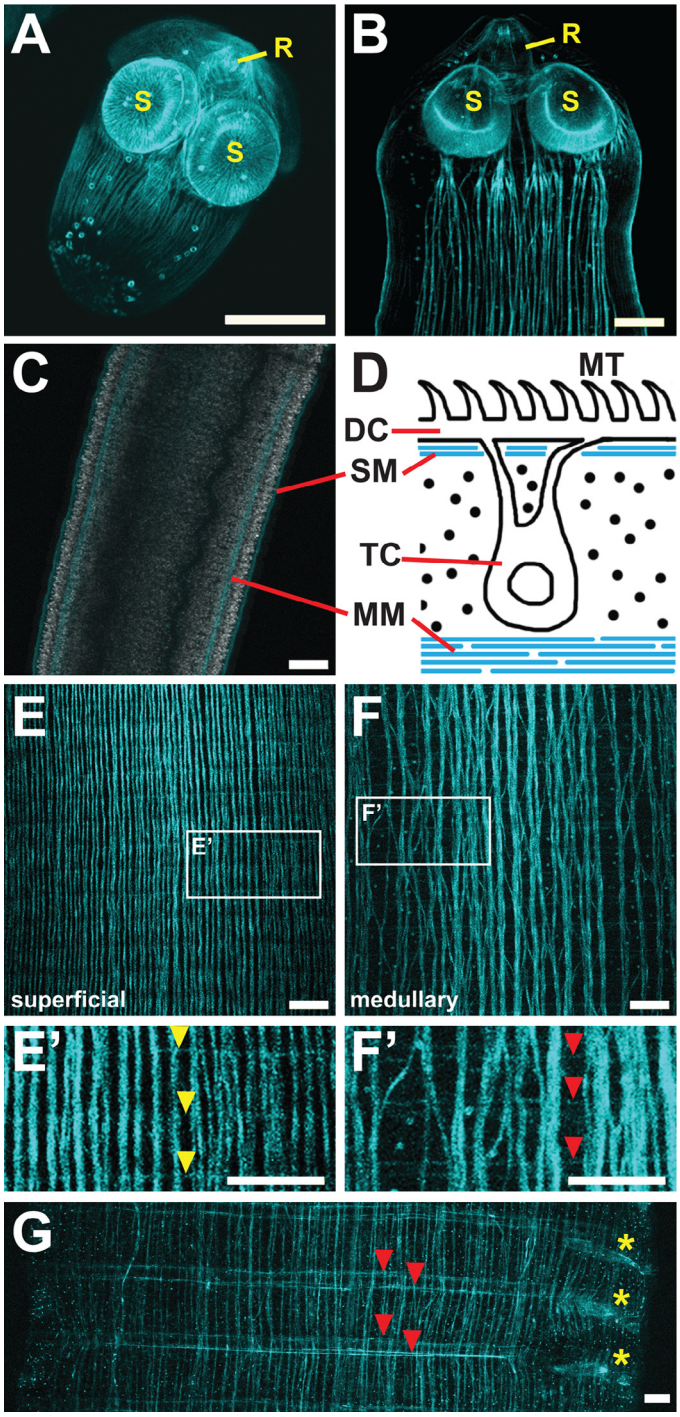

Fig. 2. Musculature. (A–G) Phalloidin staining of musculature (cyan). (A) Newly excysted juvenile tapeworm with clearly visible suckers and rostellum. (B) Scolex of an adult tapeworm. (C) Phalloidin and DAPI (gray) staining showing that superficial and medullary muscles flank the tegumentary cytons. (D) Depiction of the muscle and tegument architecture. (E) *En face* view of superficial muscle of the strobila. This is a maximum projection of the most apical fibers in an immature region of the strobila. The thickness of the projection is 4 μm. (E′) Magnified view of circular muscle fibers in the superficial layer (yellow arrowheads). (F) *En face* view of medullary muscle of the strobila. This is a maximum projection taken from the same confocal z-stack as E positioned 9 μm basal to the first visible superficial fibers. The thickness of the projection is 8 μm. (F′) Magnified view of the circular muscle fibers in the medullary layer (red arrowheads). (G) Transverse muscle fibers in the strobila primarily mark the proglottid boundaries (red arrowheads). The terminal genitalia are also highly muscularized (asterisks). Scale bars: A–F′ = 50 μm; G = 100 μm. S = sucker, R = rostellum, MT = microtriches, DC = distal cytoplasm, SM = superficial muscle, TC = tegumentary cyton, and MM = medullary muscle.

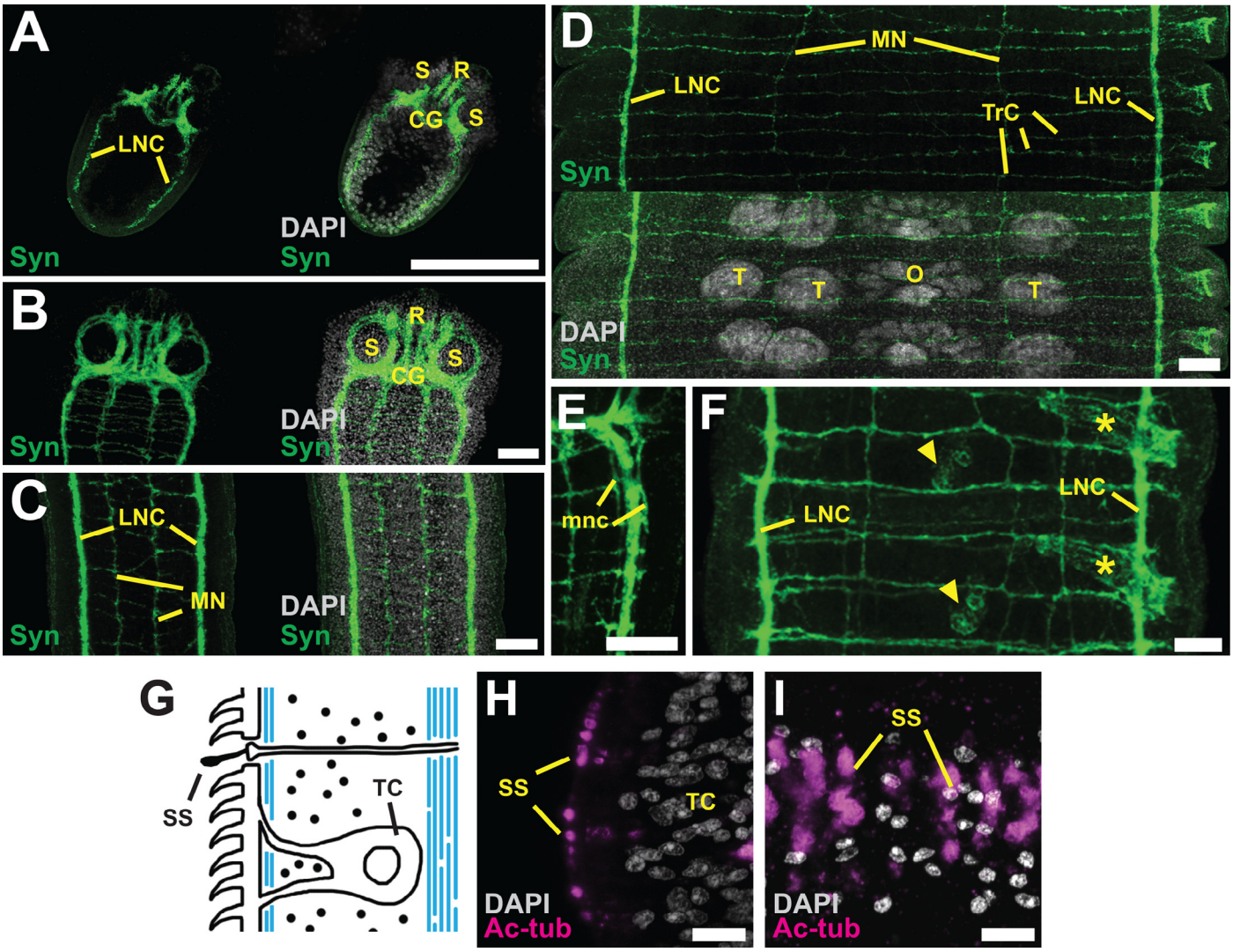

Fig. 3. Nervous and sensory system. (A–D) Progression of nervous system development visualized by anti-synapsin (Syn) staining and DAPI. (A) Newly excysted *H. diminuta* juveniles have prominent lateral nerve cords and major innervations into the suckers and rostellum. (B) The general architecture of the central nervous system is maintained in the scolex of adult *H. diminuta*. (C) The germinative region has numerous neuronal projections to and from the lateral nerve cords. Two median nerves also extend through the length of the tapeworm. (D) Once proglottidization has begun, a stereotypical pattern of three major transverse commissures per proglottid becomes established. (E) Adjacent to each lateral nerve cord lie minor nerve cords. (F) Innervation of the reproductive system occurs at poral organs including the genital atrium and cirrus pouch (asterisk) as well as the oviduct and vitelline duct (arrowhead). (G–I) Sensilla at the surface of the tegument labeled with anti-acetylated α-tubulin antibodies (Ac-tub). (G) Diagram of sensilla projecting through the tegument. (H) Cross-section view of the sensilla relative to the tegumentary cytons at the edge of a typical proglottid. (I) *En face* view of the surface of the tegument after maximum projection showing patches of sensilla. Scale bars: A–D: 100 μm; E, F: 50 μm; H, I: 10 μm. LNC = lateral nerve cord, S = sucker, R = rostellum, CG = cephalic ganglia, MN = median nerve, TrC = transverse commissures, O = ovary, T = testis, mnc = minor nerve cord, SS = sensilla, and TC = tegumentary cyton(s).

diminuta. For example, staining of acetylcholinesterase (AChE) activity reveals a series of rings in the rostellar capsule (Wilson and Schiller, 1969) that is not obvious using synapsin staining. Supplemental Movie S2 provides a frame-by-frame view of the innervations visible using synapsin staining in the adult scolex. For a detailed description of innervation in the scolex, readers are referred to excellent neurocytological descriptions using AChE (Wilson and Schiller, 1969) and paraldehyde-fuchsin (Specian and Lumsden, 1980) staining.

Throughout the strobila, the nervous system is elaborated in a highly stereotypical pattern. The longitudinal cords and nerves traverse the entire length of the strobila. Additionally, three transverse commissures connect to the lateral nerve cords in every proglottid (Fig. 3D). Peripheral nerves project throughout the parenchyma though they are more difficult to resolve using whole mount staining with synapsin antibodies. Tracing of specific nervous projections has been accomplished using high-resolution imaging of sections stained with neuronal markers like anti-serotonin sera (Webb and Mizukawa, 1985).

Under higher magnification, the fine structure of the nervous system can be revealed with synapsin staining. For example, minor nerve cords that flank the lateral nerve cords can be resolved (Fig. 3E). These structures were previously identified using staining of AChE activity (Wilson and Schiller, 1969). However, we were unable to definitively identify “motor end plates” at the neuromuscular junctions along the lateral nerve cords as was seen with AChE staining (Wilson and Schiller, 1969). Thus, synapsin antibodies are a good general marker for the nervous system but other tools may be necessary to highlight specific neuronal contacts.

The reproductive system is clearly innervated at particular points. At the poral edge, the cirrus pouch and genital atrium are strongly stained with synapsin antibodies (Fig. 3F, asterisks). Additionally,

peripheral neurons project to the oviduct and vitelline duct (Fig. 3F, arrowheads) and may play important roles in coordinating fertilization and the pairing of the zygote with a vitelline cell from the vitelline gland. Most other reproductive structures like the gonads, uterus, and sperm ducts are not stained with synapsin or other neuronal stains such as antibodies against various neurohormonal peptides or histochemistry for AChE activity (Gustafsson, 1987; Gustafsson et al., 1995; Sukhdeo and Sukhdeo, 1994; Wilson and Schiller, 1969). However, considering that neuropeptides have been shown to play important roles in the regulation of reproductive

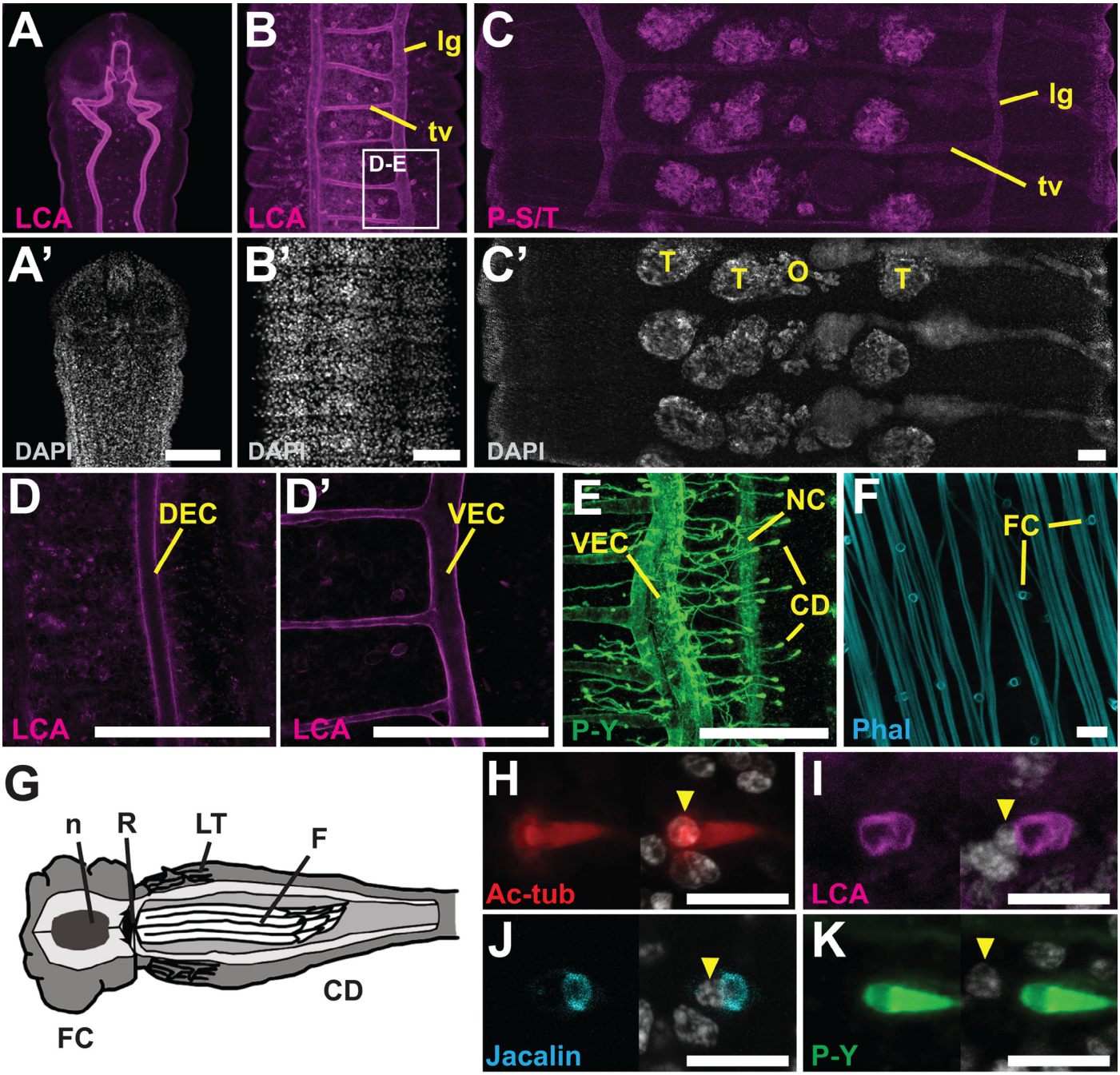

Fig. 4. Osmoregulatory system. (A–C) Excretory canals of adult *H. diminuta* can be visualized by staining with LCA and phospho-serine/threonine antibodies (P-S/T). (A′–C′) DAPI staining shows the degree of development of each proglottid. (A–A′) Adult scolex. (B–B′) Immature proglottids. (C–C′) Reproductively mature proglottids. The inset in B shows the approximate position of frames D-E (imaged from different specimens). The longitudinal canals are dorso-ventrally paired and run the length of the animal. Single transverse canals link to longitudinal canals in each proglottid. (D–D′) Confocal micrographs from a z-stack of LCA staining showing that the dorsal excretory canal is smaller than the ventral excretory canal and that only the ventral excretory canal is connected to transverse canals. (E) The canals are connected to a network of collecting ducts that terminate in flame cells. The ducts can be visualized with anti-phospho-tyrosine (P-Y) antibodies. (F) Flame cells stained with phalloidin (Phal) are distributed throughout the medullary muscle and parenchyma. (G) Depiction of flame cells and collecting ducts modified from Lumsden and Specian (1980). (H–K) High magnification view of flame cells and collecting ducts paired with DAPI labeling of nuclei (gray). The arrowheads point to the flame cell nuclei. (H) Anti-acetylated α-tubulin antibodies (Ac-tub) label the flame cell cytoplasm and the cilia that compose the flame in the collecting duct. (I) LCA labels the cytoplasm of the collecting duct directly juxtaposed to the flame cell but not the flame cell itself. (J) Jacalin stains around the rootlet that borders the flame cell and collecting duct. (K) Anti-phospho tyrosine antibodies label the collecting duct but the epitopes are largely absent in the flame cell proper. Scale bars: A–E′: 100 μm; F–K: 10 μm. lg = longitudinal, tv = transverse, O = ovary, T = testis, DEC = dorsal excretory canal, VEC = ventral excretory canal, NC = nerve cord, CD = collecting duct, FC = flame cell, n = nucleus, R = rootlet, LT = leptotriches, and F = flame/cilia.

development and function in planarians (Collins et al., 2010), it is premature to rule out innervation in these structures.

Additionally, sensory projections known as sensilla are found on the surface of the tegument as diagramed in Fig. 3G. These sensilla are ciliated, dendritic projections and can be detected by staining with anti-acetylated α-tubulin antibodies (Fig. 3H, I). Sensilla are common in many tapeworm species (Cooper et al., 1975; Morseth, 1967; Webb and Davey, 1974) and are presumed to function in chemosensation and/or mechanosensation (Lumsden and Specian, 1980).

3.4. Osmoregulatory system

Osmoregulation in *H. diminuta* is facilitated by an organ system that bears many similarities to protonephridia of other flatworms (Wilson and Webster, 1974). In adult *H. diminuta*, the osmoregulatory system is made of three major parts: (1) canals for excretion; (2) networks of capillary-like tubules; and (3) flame cells that function as primitive nephrons.

The excretory canals can be stained with *Lens culinaris* lectin (LCA), anti-phospho serine/threonine antibodies, and anti-phospho tyrosine antibodies (Fig. 4A–E). In the scolex, the excretory canals extend into the rostellum (Fig. 4A). Throughout the body of the adult, the excretory canals have a ladder-like appearance with both longitudinal and transverse canals (Fig. 4B, C). The longitudinal canals are dorso-ventrally paired and laterally positioned while a single transverse canal connects the longitudinal canals in each proglottid (Fig. 4B, C). The dorsal excretory canal (DEC) is distinguishable from the ventral excretory canal (VEC) by its smaller diameter (Fig. 4D, D′). The transverse canals are connected to the VEC only (Fig. 4D′). The canals are connected to a network of tubules that terminate with flame cells (Fig. 4E, F). The flame cells are distributed throughout the medullary muscle and parenchyma (Fig. 4F), and are directly connected to collecting ducts.

The architecture of flame cells and adjacent collecting ducts is depicted in Fig. 4G. Various stains can distinguish components of the flame cells and collecting ducts (Fig. 4H–K). Anti-acetylated α-tubulin antibodies label the flame cell and the flame/cilia that extend into the collecting duct (Fig. 4H). LCA labels the cytoplasm of the collecting duct but not the flame cell (Fig. 4I). The lectin Jacalin labels the border between the flame cell and collecting duct around the rootlet structure (Fig. 4J). Anti-phospho tyrosine antibodies label the collecting duct, including the ciliated flame but not the flame cell proper (Fig. 4K).

Flame cells are predicted to filter the body fluids of *H. diminuta* and funnel waste to the canal system through the collecting ducts. The longitudinal canals open into the most posterior proglottid and can directly release waste into the environment (Lumsden and Specian, 1980). However, excretory functions are also mediated by the tegument, which can release waste products through vesicular transport (Lumsden and Specian, 1980).

3.5. Rostellum

H. diminuta forms a hookless rostellum that can be actively maneuvered by the parasite and may aid in attachment and/or migration of the parasite along the intestinal wall. The presence of large vesicles in the rostellum suggests that it may also play secretory functions (Lumsden and Specian, 1980). The rostellum is covered by the same tegument that is contiguous with the rest of the tapeworm body. However, the rostellar surface shows differential specificity for binding of lectins. Lectins such as succinylated wheat germ agglutinin (sWGA) and peanut agglutinin (PNA) bind to the rostellar surface while lectins such as LCA do not show any specificity for this region (Fig. 5A, B). Thus the tegument at the rostellum appears to be a specialized structure. The differential specificity for lectin binding at the rostellum is already apparent in newly excysted juveniles (Fig. 5A, B) and persists in the adults (Fig. 5C).

Previous studies have found that the fine structure of the microtriches at the rostellar surface are unique, with more elongated projections and filamentous tips than microtriches on the rest of the body tegument (Lumsden and Specian, 1980). The differential specificity for lectins indicates that the carbohydrate composition of tissue at this site is different from the rest of the tegument and that the surface of the rostellum might be functionally specialized compared to the rest of the tegument.

3.6. Reproductive structures

As *H. diminuta* matures, each proglottid forms both male and female reproductive organs. In Fig. 6A, the reproductive system of *H. diminuta* is diagrammed. Sperm is made in testis lobules and is shuttled through a system of sperm ducts to a common repository called the external seminal vesicle (ESV). Sperm is then sent to the internal seminal vesicle (ISV), which is connected to the male ejaculatory organ: the cirrus (C). The cirrus can extend outside of the proglottid to penetrate a different proglottid through the female genital pore called the genital atrium (GA). Sperm is deposited into the vagina (V) and stored in the seminal receptacle (SR). Since reproductive development is protandrous in *H. diminuta*, the sperm can be stored in the SR even before the ovary has matured sufficiently to produce oocytes (Lumsden and Specian, 1980; Nollen, 1975; Roberts, 1961). Mature oocytes and sperm are trafficked to the oviduct (OD) where fertilization occurs. The zygote is then paired with a single vitelline cell that originates from the vitelline gland (VG). The vitelline gland sits atop the uterus and vitelline cells contribute to the construction of protective membranes and coats that enclose the developing embryo (Ubelaker, 1980). At early stages of development, the uterus (U) is small but it continues to grow in size as fertilization progresses to accommodate the developing embryos.

The reproductive organs of *H. diminuta* are complex but we have successfully labeled various components with lectins, antibodies, and other stains. In fact, the degree of reproductive maturity of each

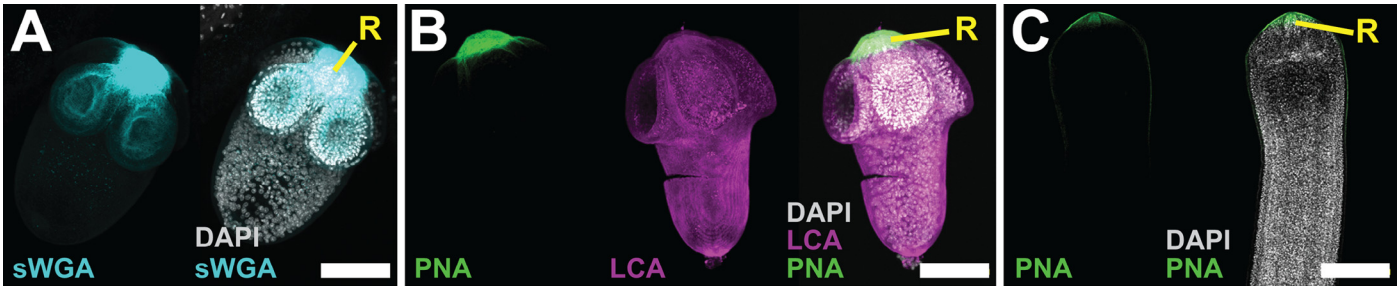

Fig. 5. Surface of the rostellum. (A, B) In newly excysted juvenile *H. diminuta*, the surface of the rostellum is a specialized region that binds lectins sWGA and PNA but not LCA. (C) Adult *H. diminuta* maintains this specialized rostellar surface shown by staining with PNA. Scale bars: A, B: 50 μm; C: 200 μm. R = rostellum.

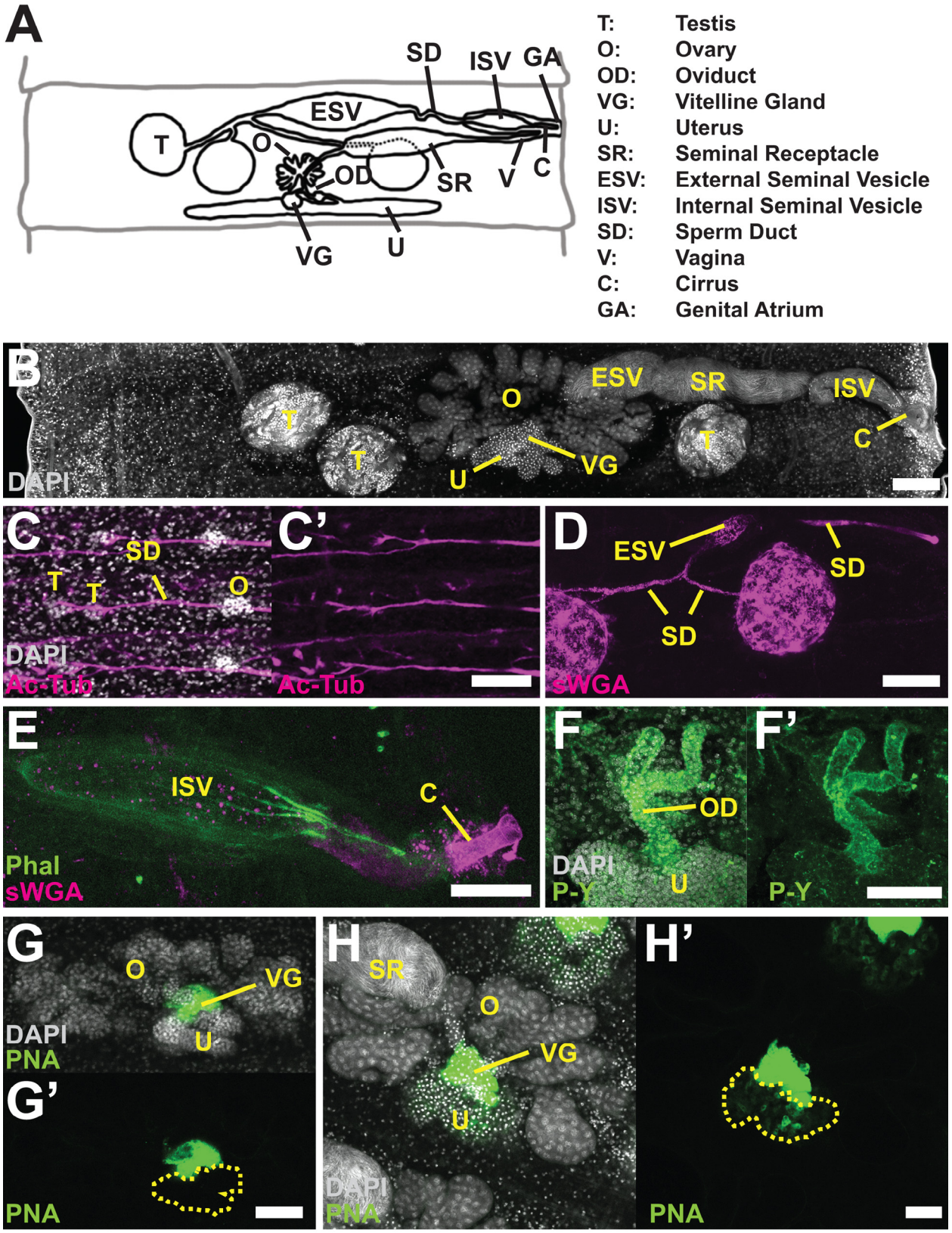

Fig. 6. Reproductive structures. (A) Depiction of reproductive tissues in mature proglottids modified from Lumsden and Specian (1980). (B) Using DAPI staining many major features of the reproductive system are plainly visualized. (C–C′) Staining with anti-acetylated tubulin (Ac-tub) antibodies labels the sperm ducts that connect the gonads and accessory reproductive organs. (D) Sperm ducts and vesicles can also be visualized using sWGA. (E) The ejaculatory organ (cirrus) is marked by sWGA and is connected to the internal seminal vesicle (labeled with phalloidin) where sperm is stored prior to penetration. (F–F′) Fertilization occurs in the oviduct, which can be labeled with anti-phospho tyrosine (P-Y) antibodies. (G–H′) The vitelline gland sits atop the uterus and is labeled by several lectins such as PNA. (G–G′) At early stages of development prior to fertilization, PNA labeling is confined to the vitelline gland. (H–H′) During fertilization, the zygote is paired with a vitelline cell as it enters the uterus. Thus at late stages, PNA labeling is also visible in the uterus (marked by the yellow dotted line). Scale bars: B: 100 μm; C–H′: 50 μm.

proglottid can be roughly visualized using a simple DAPI stain (Fig. 6B). The gonads and genital pore components are clearly visible by DAPI staining because of their distinctive morphologies (Fig. 6B). The external seminal vesicle, internal seminal vesicle, and seminal receptacle can be visualized with DAPI once they accumulate sperm (Fig. 6B).

The sperm ducts that connect the gonads and other accessory reproductive structures can be labeled with anti-acetylated α-tubulin antibodies (Fig. 6C, C′) and sWGA (Fig. 6D). sWGA also labels the cirrus and its connection to the internal seminal vesicle, which can be labeled with phalloidin (Fig. 6E). The oviduct and the branched connections to the ovary, seminal receptacle, vitelline gland, and uterus can be labeled with anti-phospho tyrosine antibodies (Fig. 6F, F′).

Using DAPI staining, the vitelline gland is difficult to distinguish because of its overlapping position with the uterus (Fig. 6B). However, it is strongly labeled by various lectins, including PNA (Fig. 6G–H'). At early stages of development, prior to fertilization, all the vitelline cells are confined to the vitelline gland (Fig. 6G′). Once fertilization occurs, vitelline cells are paired with zygotes as they enter the uterus. Thus, PNA staining becomes apparent in the uterus, which is outlined by the yellow dotted line (Fig. 6H′).

3.7. Gonads to embryos

Each proglottid stereotypically makes three testis lobules, a single centrally located ovary and copulatory organs that form at one lateral surface, which marks the "poral" edge (Fig. 7A). Typically, two testis lobules are positioned on the aporal side of the ovary and one testis lobule is positioned on the poral side on the ovary (Fig. 7A) though there is limited variation between proglottids.

The ovary is a lobate organ in which oocytes are specified. At early stages of development, the ovaries are small with few lobes and abundant cell divisions (marked by anti-phospho histone H3

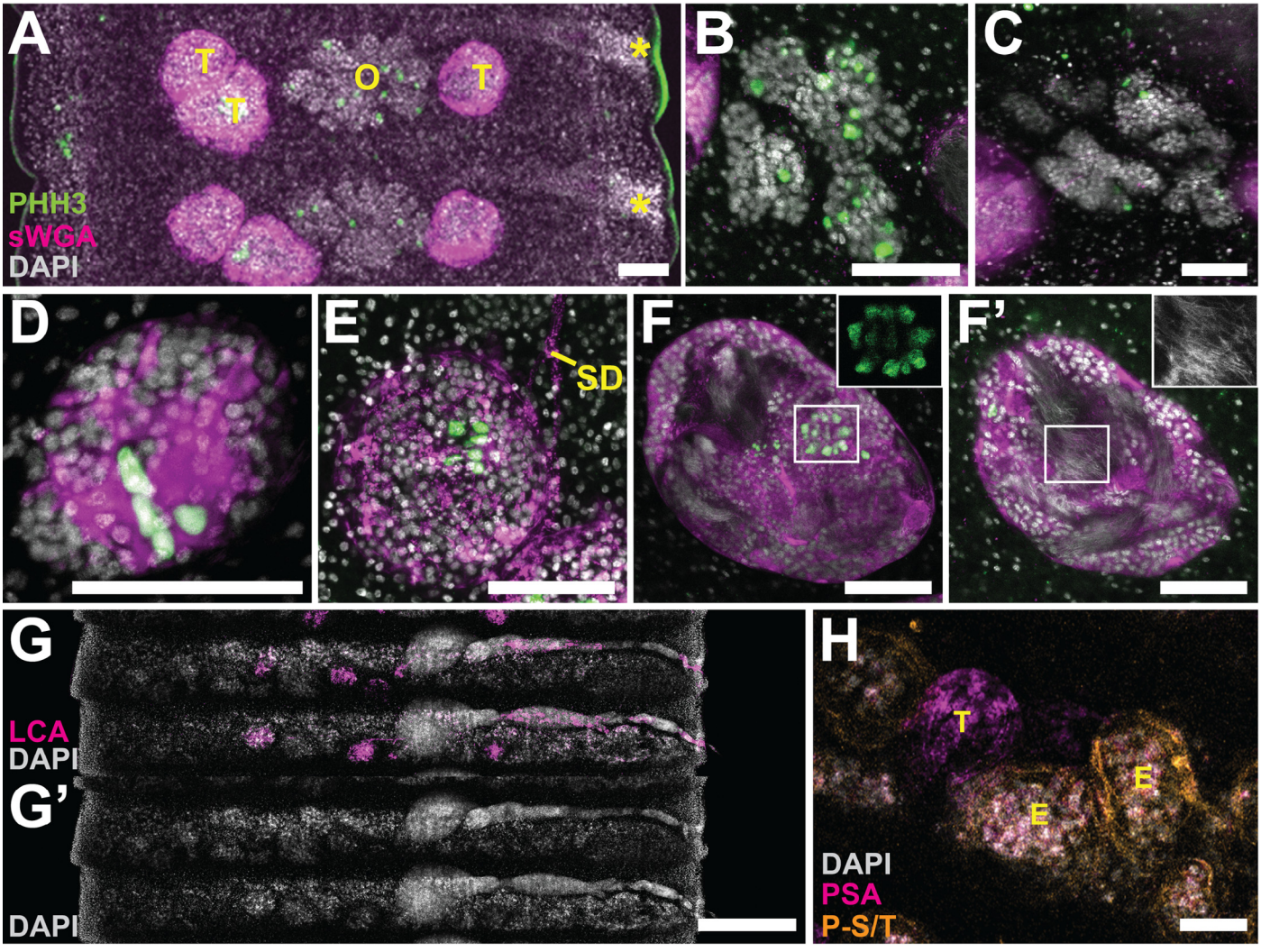

Fig. 7. Gonads and gravid proglottids. (A) Two proglottids with typical arrangement of gonads. The ovary is centrally located with two testis lobes on the aporal side and one testis lobe on the poral side. The asterisks mark the genital pore. Testes are labeled with sWGA but can also be labeled with LCA, PNA, and *Pisum sativum* agglutinin (PSA) (not shown). Mitotic cells are labeled with anti-phospho histone H3 (PHH3) antibodies; dividing germ cells are visible throughout the gonads. (B) Early ovary development. (C) Late ovary development, showing a highly lobate morphology and decreasing frequency of mitoses. (D–F) Development of testis lobules. (D) Early testes development. (E) Middle stage of testes development. (F–F′) Late stage of testes development. (F) A single confocal micrograph toward the periphery of a mature testis lobe where clusters of mitotic cells can be observed (inset). (F′) A single confocal micrograph of the same testis lobe in F toward the interior where mature sperm can be visualized in the lumen (inset). (G–G′) Low magnification view of two gravid proglottids showing degenerating gonads and accessory reproductive structures labeled with LCA. Each proglottid is taken over by an expanded uterus filled with embryos. (H) High magnification view of a gravid proglottid in which a degenerating testis lobe is marked with PSA and embryos enclosed in membranes and protective coats are labeled with anti-phospho serine/threonine (P-S/T) antibodies. Scale bars: A–F′: 50 μm; G–G′: 500 μm; H: 100 μm. T = testis, O = ovary, SD = sperm duct, and E = embryo.

staining) to give rise to the female gametes (Fig. 7B). As development progresses, the ovaries increase in size and become highly lobate while cell divisions become increasingly less frequent (Fig. 7C).

The testes also increase in size and complexity as development progresses (Fig. 7D–F′). The male gametes are formed from spermatogonial stem cells following four mitotic and two meiotic divisions to give rise to 64 spermatozoa (Kelsoe et al., 1977). Mature elongated spermatozoa have a flattened head and long tail that measure 250–300 μm (Kelsoe et al., 1977). Rosettes of 8 or 16 spermatogonia are often visible at the outer surface of the testes lobule (Fig. 7F). Mature sperm is deposited into the lumen of the testes (Fig. 7F′). This organization is reminiscent of testis architecture in the planarian *S. mediterranea* (Wang et al., 2010) though further characterization with molecular markers is needed before direct parallels can be drawn.

It is no exaggeration to say that *H. diminuta* is in a race to produce as many progeny as possible considering the challenges associated with its multi-host life cycle. As fertilization progresses, the uterus expands and is filled with developing embryos. Eventually, the reproductive structures degenerate (Fig. 7G, G′) and each proglottid is entirely taken over by the uterus. Embryos continue to divide and elaborate protective coats that can be labeled with anti-phospho serine/threonine antibodies (Fig. 7H). *H. diminuta* will then release large parts of the most posterior strobila that contain gravid proglottids through apolysis. These proglottids will then exit the rat with the stool; continuation of the life cycle hinges on suitable arthropod hosts consuming this embryo-rich excrement.

4. Conclusion

In this study, we demonstrate that common laboratory reagents can be used to specifically label different tissues and organs of *H. diminuta*. Furthermore, the tissue architecture observed using confocal microscopy concurs with previously reported descriptions of *H. diminuta* anatomy. Thus, we have developed a robust and simple protocol to observe *H. diminuta* organ structures. We hope that the developments reported here will serve as a useful resource to the community of parasitologists.

Many important questions about parasite biology can be addressed using *H. diminuta* as a model system. For example, *H. diminuta* can be used to identify and characterize parasite-specific genes that are necessary for parasite growth and reproductive health. *H. diminuta* can also be used to screen for drugs that negatively impact parasite survival. The stains we have characterized in this study will be useful to analyze phenotypes following loss-of-function perturbations in *H. diminuta* without the immediate need for specific molecular markers. This study enriches the toolbox available to researchers in the search for new anthelminthic drugs to combat the scourge of parasitic flatworm infections.

Acknowledgements

We thank Richard Davis (University of Colorado School of Medicine) for his kind and invaluable assistance in teaching TR to propagate and handle *H. diminuta*. We also thank Bo Wang, Rachel Roberts-Galbraith, and Melanie Issigonis for comments on the manuscript. PAN is an investigator of the Howard Hughes Medical Institute.

Appendix: Supplementary material

Supplementary data to this article can be found online at doi:10.1016/j.exppara.2015.05.015.

References

Bolla, R.I., Roberts, L.S., 1971. Developmental physiology of cestodes. IX. Cytological characteristics of the germinative region of *Hymenolepis diminuta*. J. Parasitol. 57, 267–277. doi:10.2307/3278024.

Brunetti, E., Kern, P., Vuitton, D.A., Writing Panel for the WHO-IWGE, 2010. Expert consensus for the diagnosis and treatment of cystic and alveolar echinococcosis in humans. Acta Trop. 114, 1–16. doi:10.1016/j.actatropica.2009.11.001.

Budke, C.M., White, A.C., Garcia, H.H., 2009. Zoonotic larval cestode infections: neglected, neglected tropical diseases? PLoS Negl. Trop. Dis. 3, e319. doi:10.1371/journal.pntd.0000319.

Chandler, A.C., 1939. The effects of number and age of worms on development of primary and secondary infections in *Hymenolepis diminuta* in rats, and an investigation into the true nature of "premunition" in tapeworm infections. Am. J. Hyg. 29, 105–114.

Chong, T., Stary, J.M., Wang, Y., Newmark, P.A., 2011. Molecular markers to characterize the hermaphroditic reproductive system of the planarian *Schmidtea mediterranea*. BMC Dev. Biol. 11, 69. doi:10.1186/1471-213X-11-69.

Collins, J.J., Hou, X., Romanova, E.V., Lambrus, B.G., Miller, C.M., Saberi, A., et al., 2010. Genome-wide analyses reveal a role for peptide hormones in planarian germline development. PLoS Biol. 8, e1000509. doi:10.1371/journal.pbio.1000509.

Collins, J.J., King, R.S., Cogswell, A., Williams, D.L., Newmark, P.A., 2011. An atlas for *Schistosoma mansoni* organs and life-cycle stages using cell type-specific markers and confocal microscopy. PLoS Negl. Trop. Dis. 5, e1009. doi:10.1371/journal.pntd.0001009.

Cooper, N.B., Allison, V.F., Ubelaker, J.E., 1975. The fine structure of the cysticercoid of *Hymenolepis diminuta*. Z. Parasitenkd 46, 229–239.

Craig, P., Ito, A., 2007. Intestinal cestodes. Curr. Opin. Infect. Dis. 20, 524–532. doi:10.1097/QCO.0b013e3282ef579e.

Cunningham, L.J., Olson, P.D., 2010. Description of *Hymenolepis microstoma* (Nottingham strain): a classical tapeworm model for research in the genomic era. Parasit. Vectors 3, 123. doi:10.1186/1756-3305-3-123.

Eckert, J., Deplazes, P., 2004. Biological, epidemiological, and clinical aspects of echinococcosis, a zoonosis of increasing concern. Clin. Microbiol. Rev. 17, 107–135.

Evans, W.S., 1980. The cultivation of *Hymenolepis* in vitro. In: Biology of the Tapeworm *Hymenolepis diminuta*. Academic Press, Inc., pp. 425–448. doi:10.1016/B978-0-12-058980-7.50011-7.

Fraguas, S., Barberán, S., Iglesias, M., Rodríguez-Esteban, G., Cebrià, F., 2014. egr-4, a target of EGFR signaling, is required for the formation of the brain primordia and head regeneration in planarians. Development 141, 1835–1847. doi:10.1242/dev.101345.

Garcia, H.H., Moro, P.L., Schantz, P.M., 2007. Zoonotic helminth infections of humans: echinococcosis, cysticercosis and fascioliasis. Curr. Opin. Infect. Dis. 20, 489–494. doi:10.1097/QCO.0b013e3282a95e39.

Gustafsson, M.K., 1987. Immunocytochemical demonstration of neuropeptides and serotonin in the nervous systems of adult *Schistosoma mansoni*. Parasitol. Res. 74, 168–174.

Gustafsson, M.K., Fagerholm, H.P., Halton, D.W., Hanzelová, V., Maule, A.G., Reuter, M., et al., 1995. Neuropeptides and serotonin in the cestode, *Proteocephalus exiguus*: an immunocytochemical study. Int. J. Parasitol. 25, 673–682.

Kelsoe, G.H., Ubelaker, J.E., Allison, V.F., 1977. The fine structure of spermatogenesis in *Hymenolepis diminuta* (Cestoda) with a description of the mature spermatozoon. Z. Parasitenkd 54, 175–187.

King, R.S., Newmark, P.A., 2013. In situ hybridization protocol for enhanced detection of gene expression in the planarian *Schmidtea mediterranea*. BMC Dev. Biol. 13, 8. doi:10.1186/1471-213X-13-8.

Lumsden, R.D., 1975a. Surface ultrastructure and cytochemistry of parasitic helminths. Exp. Parasitol. 37, 267–339.

Lumsden, R.D., 1975b. The tapeworm tegument: a model system for studies on membrane structure and function in host–parasite relationships. Trans. Am. Microsc. Soc. 94, 501–507.

Lumsden, R.D., Byram, J., 1967. The ultrastructure of cestode muscle. J. Parasitol. 53, 326–342.

Lumsden, R.D., Specian, R., 1980. The morphology, histology, and fine structure of the adult stage of the cyclophyllidean tapeworm *Hymenolepis diminuta*. In: Biology of the Tapeworm *Hymenolepis diminuta*. Academic Press, Inc, pp. 157–280. doi:10.1016/B978-0-12-058980-7.50008-7.

Morseth, D.J., 1967. Observations on the fine structure of the nervous system of *Echinococcus granulosus*. J. Parasitol. 53, 492–500.

Nollen, P.M., 1975. Studies on the reproductive system of *Hymenolepis diminuta* using autoradiography and transplantation. J. Parasitol. 61, 100–104.

Olson, P.D., Zarowiecki, M., Kiss, F., Brehm, K., 2012. Cestode genomics – progress and prospects for advancing basic and applied aspects of flatworm biology. Parasite Immunol. 34, 130–150. doi:10.1111/j.1365-3024.2011.01319.x.

Pouchkina-Stantcheva, N.N., Cunningham, L.J., Hrčkova, G., Olson, P.D., 2013. RNA-mediated gene suppression and in vitro culture in *Hymenolepis microstoma*. Int. J. Parasitol. 43, 641–646. doi:10.1016/j.ijpara.2013.03.004.

Roberts, L.S., 1961. The influence of population density on patterns and physiology of growth in *Hymenolepis diminuta* (Cestoda:Cyclophyllidea) in the definitive host. Exp. Parasitol. 11, 332–371.

Roberts, L.S., 1980. Development of *Hymenolepis diminuta* in its definitive host. In: Biology of the Tapeworm *Hymenolepis diminuta*. Academic Press, Inc., pp. 357–423. doi:10.1016/B978-0-12-058980-7.50010-5.

Rothman, A.H., 1959. Studies on the excystment of tapeworms. Exp. Parasitol. 8, 336–364.

Siles-Lucas, M., Hemphill, A., 2002. Cestode parasites: application of in vivo and in vitro models for studies on the host-parasite relationship. Adv. Parasitol. 51, 133–230.

Specian, R.D., Lumsden, R.D., 1980. The microanatomy and fine structure of the rostellum of *Hymenolepis diminuta*. Z. Parasitenkd 63, 71–88.

Sukhdeo, S.C., Sukhdeo, M.V., 1994. FMRFamide-related peptides in *Hymenolepis diminuta*: immunohistochemistry and radioimmunoassay. Parasitol. Res. 80, 374–380.

Tsai, I.J., Zarowiecki, M., Holroyd, N., Garciarrubio, A., Sanchez-Flores, A., Brooks, K.L., et al., 2013. The genomes of four tapeworm species reveal adaptations to parasitism. Nature 496, 57–63. doi:10.1038/nature12031.

Ubelaker, J.E., 1980. Structure and ultrastructure of the larvae and metacestodes of *Hymenolepis diminuta*. In: Biology of the Tapeworm *Hymenolepis diminuta*. Academic Press, Inc., pp. 59–156. doi:10.1016/B978-0-12-058980-7.50007-5.

Voge, M., Heyneman, D., 1957. Development of *Hymenolepis nana* and *Hymenolepis diminuta* (Cestoda: Hymenolepididae) in the intermediate host *Tribolium confusum*. Univ. Calif. Publ. Zool. 59, 549–580.

Wang, Y., Stary, J.M., Wilhelm, J.E., Newmark, P.A., 2010. A functional genomic screen in planarians identifies novel regulators of germ cell development. Genes Dev. 24, 2081–2092. doi:10.1101/gad.1951010.

Webb, R.A., Davey, K.G., 1974. Ciliated sensory receptors of the unactivated metacestode of *Hymenolepis microstoma*. Tissue Cell 6, 587–598.

Webb, R.A., Mizukawa, K., 1985. Serotoninlike immunoreactivity in the cestode *Hymenolepis diminuta*. J. Comp. Neurol. 234, 431–440. doi:10.1002/cne.902340403.

Wellcome Trust Sanger Institute, 2014. Parasitic worm genomes: largest-ever dataset released. <http://www.sanger.ac.uk/about/press/2014/141128.html> (accessed 12.02.14).

Wilson, R.A., Webster, L.A., 1974. Protonephridia. Biol. Rev. Camb. Philos. Soc. 49, 127–160.

Wilson, V.C., Schiller, E.L., 1969. The neuroanatomy of *Hymenolepis diminuta* and *H. nana*. J. Parasitol. 55, 261–270.

Zayas, R.M., Cebrià, F., Guo, T., Feng, J., Newmark, P.A., 2010. The use of lectins as markers for differentiated secretory cells in planarians. Dev. Dyn. 239, 2888–2897. doi:10.1002/dvdy.22427.